

Gravitational Lensing & Stellar Dynamics

Dark-Matter and Baryons in Early-type Galaxies to $z=1$

L.V.E. Koopmans^{*†}

Kapteyn Institute, P.O. Box 800, 9700AV Groningen, The Netherlands

E-mail: koopmans@astro.rug.nl

Gravitational lensing and stellar dynamics provide two complementary, nearly orthogonal, constraints on the mass distribution of early-type lens galaxies. This allows the luminous and dark-matter distribution in higher-redshift ($z > 0.1$) galaxies to be studied beyond the limitations of each individual method. Two surveys have been initiated to compile a large sample of early-type galaxies suitable to lensing and dynamical studies: (1) The Lenses Structure & Dynamics (LSD) Survey and (2) the Sloan Lens ACS (SLACS) Survey.

Using spherically symmetric mass models, I illustrated how lensing and dynamical constraints can be used to measure the “effective” density slope (γ') of galaxies inside their Einstein radii and estimate the typical error on this determination.

The main results from the LSD survey thus far are: (i) Massive (typically $> L_*$) early-type galaxies at $z \approx 0.5-1$ contain a significant fraction $f_{\text{CDM}} = 0.4 - 0.7$ of dark matter inside their Einstein radii. [The null-hypothesis, $f_{\text{CDM}} = 0$, is excluded at the $> 99\%$ in all analyzed systems.] (ii) The inner CDM density slope is $\gamma_{\text{CDM}} = 1.3^{+0.2}_{-0.3}$ (68% CL) for $\rho_{\text{CDM}} \propto r^{-\gamma_{\text{CDM}}}$. (iii) The total density slope $\gamma' = 1.9 \pm 0.1$ (with 0.3 rms scatter in the sample; $\rho \propto r^{-\gamma'}$). The intrinsic scatter of 15% in γ' is consistent with local dynamical studies and can lead to a 30% rms scatter in inferred values of H_0 from lens time-delays, when purely isothermal mass models are assumed.

Hence, the common practice to assume that lens galaxies are perfectly isothermal should be abandoned, especially in cases where this assumption is critical.

Baryons in Dark Matter Halos

5-9 October 2004

Novigrad, Croatia

^{*}Speaker.

[†]A footnote may follow.

1. Introduction

Whereas the standard cosmological model (Λ CDM) is very successful in the linear regime, in the non-linear regime observations and theory appear to diverge. First, the inner mass profiles of dwarf and LSB galaxies – which are thought to be dominated by cold dark matter – appear to have cores with $\gamma_{\text{CDM}} < 1.0$ ($\rho \propto r^{-\gamma_{\text{CDM}}}$), much flatter than the predicted $\gamma_{\text{CDM}}=1.0-1.5$. Second, the predicted amount of dark-matter substructure in galaxy halos is not reflected by the amount of visible substructure seen around the Milky Way.

Although this might herald trouble for the standard cosmological model on small scales, one ‘pillar’ of the hierarchical structure formation model has yet to be studied in detail beyond the local Universe: massive early-type galaxies. Although Fundamental Plane studies of their stellar-population evolution have been done to $z \sim 1$, comparatively little is known about their internal mass structure and their evolution. Since early-type galaxies are predicted to form at the highest density peaks in the early Universe, one expects them to form with significant amounts of cold dark matter. Hence knowledge of their dark-matter halos, their formation and their subsequent evolution provide crucial tests of the Λ CDM model.

Studying the internal mass distribution of early-type galaxies is challenging, not only because baryonic collapse changes the initial dark-matter mass distribution, but also because simple rotation curves – as for disk galaxies – can often not be obtained and stellar-dynamical or gravitational-lensing studies on their own suffer from degeneracies between isotropy, mass and mass profile. Consequently, the number of low-redshift early-type galaxies known to have or not have dark-matter is relatively small and less is known either about the shape of their inner dark-matter density profiles, let alone about early-type galaxies at higher redshifts or their structural evolution. Whereas lensing also provides some constraints on dark-matter halos, its distribution can also often not be measured because of the well-known mass-profile degeneracy.

However, determining the amount, distribution and evolution of baryonic (e.g. stellar) and dark matter in the inner ~ 15 kpc of early-type galaxies is a crucial step in shedding light on (i) the Λ CDM model, (ii) the formation scenario(s) of the most massive galaxies in the Universe and (iii) the interaction between baryonic and dark matter in galaxy formation (e.g. collisionless if stars formed before galaxy formation, or collisional if stars formed during galaxy formation). It is therefore essential to break degeneracies in the existing techniques and more precisely measure the inner mass profiles of early-type galaxies up to $z \sim 1$.

The reader is referred to Kochanek, Schneider & Wambsganss (2004) for a thorough introduction in the above issues, that are related to lensing. In this proceeding, I try explain in more detail why lensing and stellar-dynamical constraints break degeneracies in mass models and then show how this technique is being applied to real galaxies.

2. Gravitation Lensing & Stellar Dynamics

In strong gravitational lenses (i.e. multiple images), the mass enclosed by the images is nearly independent from the assumed mass model of the lens and can often be determined to less than a few percent accuracy. The weak dependence on higher-order moments of the mass distribution also implies that it is difficult to measure the mass profile of a lens galaxy, leading to the *radial mass*

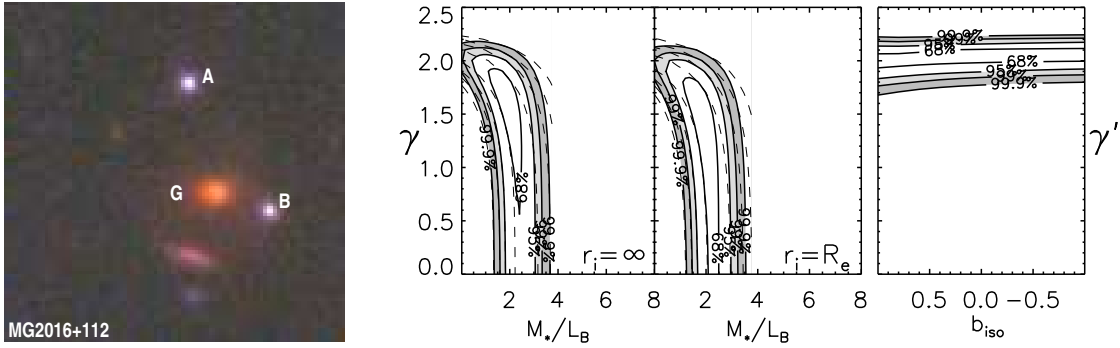


Figure 1: Left figure: HST true-color image of MG2016+112 at $z=1.004$. Right figure: Likelihood contours in the plane of stellar M_*/L_B versus dark-matter slope (γ) for the isotropic/anisotropic velocity ellipsoid with an Osipkov–Merritt anisotropy radius of $r_i = \infty/R_e$. The total M_{tot}/L_B inside the Einstein radius is $8.0 M_\odot/L_{\odot,B}$, much larger than the stellar $M_*/L_B = 2.2 \pm 0.3 M_\odot/L_{\odot,B}$, indicating an extended massive dark-matter halo. Note that the resulting total (luminous+dark-matter) mass slopes (γ' ; $\rho_{tot} \propto r^{-\gamma'}$) is nearly independent from the (constant) anisotropy parameter b_{iso} .

profile degeneracy (e.g. Wucknitz 2002). This degeneracy, although not exact, is closely related to the mass-sheet degeneracy. The radial mass profile can also be determined by comparing the kinematic profiles (e.g. stellar dispersion) with those inferred from mass models. However, the same (luminosity weighted) stellar velocity dispersion can be the result of more a shallow/steep mass profile with radial/tangential anisotropy of the stellar velocity ellipsoid, especially if also the enclosed mass is allowed to vary. Hence, there is the well-known *mass–anisotropy degeneracy*.

Because gravitational lensing determines the enclosed mass of the lens accurately, this is precisely what is needed in stellar dynamics to break the degeneracy with the mass profile and anisotropy as recently shown (see Treu & Koopmans 2004 and references therein).

2.1 Spherically Symmetric Lensing & Dynamical Models

Why does the combination of stellar dynamics and gravitational lensing work so well in determining the mass-density slope of lens galaxies? To answer this question, the stellar velocity dispersion profile is derived for power-law models (in density, luminosity density, etc.) and for constant stellar velocity-ellipsoid anisotropy (i.e. β models). It follows that all derived quantities then obey equally simple power-law scaling relations. Realistic galaxies are of course more complex. However, it serves to illustrate how different galaxies properties are interrelated and why mass-model degeneracies can be broken. They also allow simple error estimates of the derived quantities.

2.1.1 Stellar Velocity Dispersion Relations

Let us suppose that the stellar component has a luminosity density $v_l(r) = v_{l,o} r^{-\delta}$ and is a trace component embedded in a total (i.e. luminous plus dark-matter) mass distribution with a density $v_p(r) = v_{p,o} r^{-\gamma}$. In addition, let us assume that the anisotropy of the stellar component $\beta = 1 - (\sigma_\theta^2/\sigma_r^2)$ is constant with radius. For a lens galaxy with a projected mass M_E inside the Einstein radius R_E , the luminosity weighted average line-of-sight velocity dispersion inside an aperture R_A

is given, after solving the spherical Jeans equations, by

$$\langle \sigma_{||}^2 \rangle (\leq R_A) = \frac{1}{\pi} \left[\frac{GM_E}{R_E} \right] f(\gamma', \delta, \beta) \times \left(\frac{R_A}{R_E} \right)^{2-\gamma'} \quad (2.1)$$

with

$$f(\gamma', \delta, \beta) = 2\sqrt{\pi} \left(\frac{\delta-3}{(\xi-3)(\xi-2\beta)} \right) \times \left\{ \frac{\Gamma[(\xi-1)/2]}{\Gamma[\xi/2]} - \beta \frac{\Gamma[(\xi+1)/2]}{\Gamma[(\xi+2)/2]} \right\} \times \left\{ \frac{\Gamma[\delta/2]\Gamma[\gamma'/2]}{\Gamma[(\delta-1)/2]\Gamma[(\gamma'-1)/2]} \right\} \quad (2.2)$$

with $\xi = \gamma' + \delta - 2$. Similarly,

$$\sigma_{||}^2(R) = \frac{1}{\pi} \left[\frac{GM_E}{R_E} \right] \left(\frac{\xi-3}{\delta-3} \right) f(\gamma', \delta, \beta) \times \left(\frac{R}{R_E} \right)^{2-\gamma'}. \quad (2.3)$$

In the simple case of a SIS with $\gamma' = \delta = \xi = 2$ and $\beta = 0$, we recover the well-known result

$$\sigma_{||}^2(R) = \frac{1}{\pi} \left[\frac{GM_E}{R_E} \right] \quad (\text{SIS}). \quad (2.4)$$

From eqn.2.1, one sees that the radial dependence of the stellar velocity dispersion depends on γ' only. All other parameters (i.e. δ , β , etc.) only enter into the normalization. Since the luminosity density (i.e. δ) is given by the observations, as is M_E from lensing, the measurement of $\langle \sigma_{||}^2 \rangle (\leq R_A \approx R_E)$ immediately gives the density slope $\gamma'(\beta)$ (where β in general plays only a minor role). *This is the basis of combining stellar dynamics with gravitational lensing.*

2.1.2 Error estimate on the mass density slope

One of the most interesting parameters to determine is γ' , i.e. the slope of the total mass density. We can estimate the change $\delta\gamma'$ from the observables. One finds to first order (assuming fixed values of β and δ):

$$\frac{\delta\sigma_{||}}{\sigma_{||}} (\leq R_A) = \frac{1}{2} \frac{\delta M_E}{M_E} + \frac{1}{2} \left(\frac{\partial \log f}{\partial \log \gamma'} - \gamma' \log \left[\frac{R_A}{R_E} \right] \right) \cdot \frac{\delta\gamma'}{\gamma'} \equiv \frac{1}{2} \left(\frac{\delta M_E}{M_E} + \alpha_g \frac{\delta\gamma'}{\gamma'} \right). \quad (2.5)$$

The second term in this equation was already derived in Treu & Koopmans (2002). If we further assume the errors on M_E and $\sigma_{||}$ to be independent,

$$\langle \delta_{\gamma'}^2 \rangle \approx \alpha_g^{-2} \left\{ \langle \delta_{M_E}^2 \rangle + 4 \langle \delta_{\sigma_{||}}^2 \rangle \right\}, \quad (2.6)$$

where $\delta_{...}$ indicate fractional errors. Since in general $\delta_{M_E} \ll \delta_{\sigma_{||}}$, one finds the simple rule of thumb that the error $\delta_{\gamma'} \sim \delta_{\sigma_{||}}$ for close-to-isothermal mass models, since $\alpha_g \sim 2$. This estimate is in very good agreement with the results from properly solving the Jeans equations for two-component mass models and justifies neglecting the mass errors (Treu & Koopmans 2004). The result differs from Kochanek (2004), who uses R_{vir} instead of R_A and does not account for the mass term or the first term in α_g . Since $\sigma_{||}$ is measured inside $R_A \leq R_E$, not inside $R_A \approx R_{\text{vir}} \gg R_E$, the real error $\delta_{\gamma'}$ inside R_E is smaller by a factor of a few than the error suggested by Kochanek (2004), as supported by the numerical models (Treu & Koopmans 2004).

2.1.3 The mass-sheet degeneracy and the Hubble Constant

The mass-sheet degeneracy, $\kappa \leftrightarrow (1 - \kappa_c)\kappa + \kappa_c$, leaves all lensing observables, except for the time-delays (for a given value of H_0), invariant. The combination of gravitational lensing and stellar dynamics provides a way to break this degeneracy.

First, we introduce two types of mass-sheets: (i) the *internal mass sheet*, i.e. a constant (or very extended) mass component that effectively acts as a mass sheet *and* is physically associated with the lens galaxy (thereby affecting its stellar dynamics), and (ii) the *external mass sheet*, i.e. a constant mass component that is present in the direction of the lens galaxy, but not physically associated (e.g. a nearly constant density of a nearby cluster or group).

In the case of the *internal mass sheet*, it is clear that stellar dynamics breaks this lensing degeneracy. A positive mass-sheet ($\kappa_c > 0$) lowers the average density slope inside the Einstein radius (R_E), whereas the total enclosed mass remains the same. This lowers stellar velocity dispersion and thus a lower density slope measured from the lensing plus dynamical models. Thus, even though lensing can *never* break the degeneracy in the true mass slope, in combination with stellar dynamics it does. In the case of the *external mass sheet*, the mass inside the Einstein radius physically associated with the lens galaxy is overestimated by $1/(1 - \kappa_c)$. Hence, the true mass of the galaxy is actually different than inferred from lensing by $\delta_{M_E} \approx -\kappa_c$. Similarly, the true mass slope, inferred from stellar dynamics as above, will be different from the true value by $\delta_\gamma \approx +\kappa_c \alpha_g^{-1}$. Since the change in time-delay is $\delta_{\Delta t} \propto (\delta_{M_E} + \gamma' \delta_\gamma / (\gamma' - 1)) \propto \kappa_c (\gamma' (\gamma' - 1)^{-1} / \alpha_g - 1)$ then the effects on H_0 tend to be opposite for $\gamma' \approx 2$. In other words, an unknown mass sheet (i.e. not accounted for in the mass model) leads to an overestimate of H_0 for a fixed γ' . However, the observed value of $\sigma_{||}$ is too small for that values of γ' and forces one to lower the latter, consequently lowering the inferred value of H_0 again.

It should be emphasized, however, that the level of cancellation for external mass sheets depends on the precise model and the cancellation is neither precise nor guaranteed.

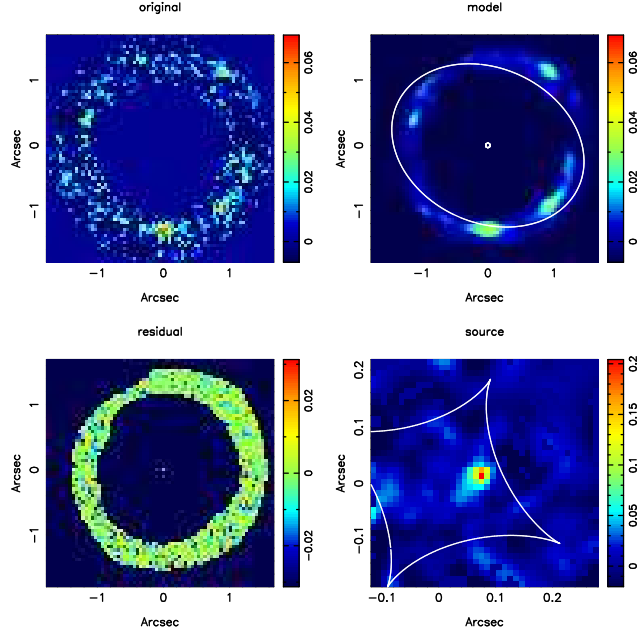
3. Observational Programs

Currently two main programs to combine gravitational lensing and stellar dynamical constraints are underway: (i) The Lenses Structure and Dynamics (LSD) Survey and (ii) the Sloan Lens ACS (SLACS) Survey. In the next two subsection, I describe each of these surveys and their results in more details. Whereas the LSD survey has concentrated thus far of early-type galaxies at $z > 0.5$, the SLACS survey is limited to galaxies at $z < 0.5$. Their combination could provide constraint on the evolution of the internal mass structure of early-type in the latter half of the age of the Universe.

3.1 The Lenses Structure & Dynamics Survey – LSD

The first target of the *Lenses Structure & Dynamics* LSD survey, the lens system MG2016+112, is shown in Fig.1, as an example, consisting of a massive elliptical galaxy (G) at $z=1.004$, multiply imaging a quasar at $z=3.273$ in two images (A & B). An 8.5-hr Keck ESI spectrum was obtained from which the stellar dispersion was determined ($\sigma = 304 \pm 27$ km/s). Given the mass enclosed by the images – determined from the lens model – one can calculate the velocity dispersion profile of the lens galaxy, with the inner dark-matter mass slope (γ with $\rho_{\text{dm}} \propto r^{-\gamma}$) and stellar mass-to-light ratio (M_*/L_B) as free parameters in a two-component luminous plus dark-matter mass model

Figure 2: Gravitational-lens inversion of SDSSJ1402, showing the galaxy-subtracted HST-ACS F435W image (upper left) within a suitable annulus. The best-model of the system (upper right) is the mapping of the source model (lower right) on to the image plane using the best-fit SIE mass model. The critical curves and caustics are plotted on the image and source models, respectively. [From Bolton et al. 2004b]



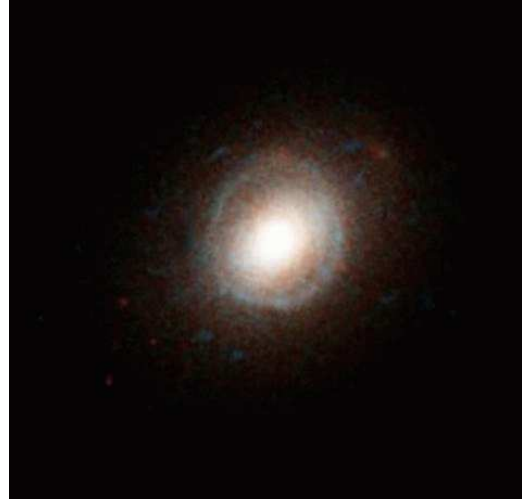
(Treu & Koopmans 2002). A useful simplification is to model the luminous *plus* dark-matter with a single density profile with slope γ' . By comparing the model and the observed kinematic profiles, one can place likelihood constraints on the values of M_*/L_B , γ_{CDM} and γ' , as illustrated in Fig. 1. We have now analyzed the dark-matter and total density profiles of five early-type galaxies between $z \approx 0.5$ and 1.0 (Treu & Koopmans 2004). Based on the constraints from the current sample, we find the following results: (i) All five early-type galaxies have massive dark-matter halos ($>99\%$ CL) with mass fractions of 40–70% inside their Einstein radius. (ii) The inner dark-matter slope is $\gamma_{\text{CDM}} = 1.3^{+0.2}_{-0.3}$ (isotropic model) and the total mass slope is $\langle \gamma' \rangle = 1.90$ with 0.30 rms if we include two more analyzed systems. (iii) The stellar mass-to-light ratio from the Fundamental Plane and from lensing & dynamics agree and lead to an evolution of $d \log(M/L_B)/dz = -0.72 \pm 0.10$.

The results presented above are very promising, since no limits on the dark-matter halos of early-type galaxies were known before at this level of accuracy or at $z > 0.1$. It shows that the technique of combining lensing & dynamics works well even for early-type galaxies at $z \approx 1$. It also shows that early-type galaxies exhibit a variety or spread of internal properties (i.e. not all galaxies are formed equal). This emphasizes the need to study more galaxies, covering a larger range of parameters space in redshift, luminosity, color, etc. in order to examine possible trends, parameter-correlations and/or evolution in more detail.

3.2 The Sloan Lens ACS Survey – SLACS

To increase the sample of lens galaxies suitable for lensing and dynamical studies, we initiated a new HST snapshot program during Cycle–13 (SNAP–10174; PI Koopmans): *the Sloan Lens ACS Surveys (SLACS)*. SLACS aims to target the 49 strong-lens candidates identified by Bolton et al. (2004a), who analyzed $\approx 50,000$ spectra from the Luminous Red Galaxy (LRG) sample from the Sloan Digital Sky Survey (SDSS). The candidates are massive early-type galaxies whose spectra show ≥ 3 nebular emission lines at a redshift higher than that of the LRG, indicating a potentially

Figure 3: A newly discover SLACS lens system. A true-color image is shown of the red lens galaxy plus a blue Einstein ring. The image was created from two single 7-min HST-ACS images in the F814W and F435W filters [Credit: L. Moustakas].



lensed star-forming galaxy within the 3-arcsec diameter spectroscopic fiber.

Bolton et al. (2004a) calculated that ≈ 20 of these candidates will be strong lenses, potentially tripling the current sample of lens systems suitable for lensing and dynamics analyzes (including LSD lenses). Since august 2004, one target has been observed each week on average in the F814W and F435W filters. Thus far about half of the sample has been targeted and $\geq 50\%$ are genuine lens systems (e.g. Figures 2 & 3).

The sample of SLACS lenses is ideal for detailed kinematic analyzes of their lens galaxies. Because of the sample selection, the lens galaxies are all bright LRGs and the lensed images are relatively faint (see Figure 3). This contrasts sharply with the majority of known lenses, where the lensed sources are bright QSOs (or galaxies) that outshine the lens galaxy itself, complicating any kind of detailed kinematic follow-up.

To study trends and evolution of the internal structure of early-type galaxies, we intend to measure the spatially resolved stellar kinematics of *individual* lens galaxies. Even for a small sample this already provides extremely interesting results (see Section 3.1), hard to obtain otherwise for galaxies beyond $z \sim 0.1$. However, a large sample of early-type galaxies with detailed determinations of their internal structure also allows one to *compare* galaxies with different masses and as function of time, to study trends and evolution.

In particular, with the anticipated sample of ≈ 30 lens galaxies (including the nine observed within the LSD survey), a detailed study of the properties and cosmic evolution of the dark-matter halos around early-type galaxies can be made. Assuming the current average numbers of $\gamma' \approx 1.9$ with 0.3 rms scatter, the $\delta_{\gamma'}$ and its rms are $15\%/\sqrt{N}$ and $30\%/\sqrt{N/2}$, respectively, per bin with N galaxies. To distinguish changes of 10% in γ' at the 2- σ level between bins, one needs 15 objects per bin. This would allow a measurement of the average and rms scatter *per bin* at the 4% and 10% accuracy level, respectively. Similarly, a total of 30 early-type lens galaxies would give the average *dark-matter* mass slope to 10% accuracy.

With an expected sample of ~ 30 LSD + SLACS early-type lens galaxies, changes with redshift (or mass) in γ' at a 10% level can potentially be detected!

4. Summary & Conclusions

The combination of stellar dynamics and gravitational lensing is starting to become a prominent tool in determining the luminous and dark-matter mass distribution in early-type galaxies beyond the local Universe. The reason is simple: stellar dynamics and gravitational lensing provide unique, nearly-orthogonal, constraints on the mass distribution of galaxies. This allows one to break degeneracies in their mass models, even with modest imaging and spectroscopic data-quality.

For example, the density slope (γ') of galaxies inside the Einstein radius ($\sim 5\text{--}15$ kpc) can be determined with an accuracy of $\delta\gamma' \sim \delta\sigma_{||}/\sigma_{||} \sim 0.1$ (for typical data-sets). Similarly, although less precisely, can one determine the fraction of dark-matter (f_{CDM}) inside the Einstein radius and its inner slope (γ_{CDM}). Results from the LSD survey thus far give: $\gamma' = 1.9 \pm 0.1$ (with rms intrinsic scatter of 0.3, for the LSD sample plus B1608+656 and PG1115+080), $\gamma_{\text{CDM}} = 1.3^{+0.2}_{-0.3}$ (68% CL) and $f_{\text{CDM}}(< R_E) = 0.4 - 0.7$ (e.g. Treu & Koopmans 2004).

The SLACS survey – a cycle-13 HST-ACS snapshot program – is yielding the anticipated (see Bolton et al. 2004a,b) large numbers of lens systems at $z \leq 0.5$, suitable for detailed lensing and dynamical analyzes. The rate of discovery promises to deliver the several dozen lens systems required to quantify the total density profile of early-type galaxies, as well as their CDM mass fraction and slope.

These measurement are expected to provide direct constraints on (Λ CDM) galaxy-formation models, which properly include dark matter, baryons and radiative processes.

References

- [1] Bolton, A. S., Burles, S., Schlegel, D. J., Eisenstein, D. J., Brinkmann, J. 2004a. Sloan Digital Sky Survey Spectroscopic Lens Search. I. Discovery of Intermediate-Redshift Star-forming Galaxies behind Foreground Luminous Red Galaxies. *Astronomical Journal* 127, 1860-1882
- [2] Bolton, A.S., Burles, S., Koopmans, L.V.E., Treu T., Moustakas, L.A. 2004b SDSSJ140228.22+632133.3: A New Spectroscopically Selected Gravitational Lens, *Astrophysical Journal Letters*, submitted, astro-ph/0410425
- [3] Kochanek, C.S., Schneider, P., Wambsganss, J., 2004, Gravitational Lensing: Strong, Weak & Micro, Proceedings of the 33rd Saas-Fee Advanced Course, G. Meylan, P. Jetzer & P. North, eds. (Springer-Verlag: Berlin)
- [4] Kochanek, C.S. 2004. Where Does The Dark Matter Begin? To appear in 'The Impact of Gravitational Lensing on Cosmology' (IAU 225), Y. Mellier and G. Meylan, eds, astro-ph/0412089
- [5] Treu, T., Koopmans, L. V. E. 2002. The Internal Structure and Formation of Early-Type Galaxies: The Gravitational Lens System MG 2016+112 at $z = 1.004$. *Astrophysical Journal* 575, 87-94
- [6] Treu, T., Koopmans, L. V. E. 2004. Massive Dark Matter Halos and Evolution of Early-Type Galaxies to $z \sim 1$. *Astrophysical Journal* 611, 739-760.
- [7] Wucknitz, O. 2002. Degeneracies and scaling relations in general power-law models for gravitational lenses. *Monthly Notices of the Royal Astronomical Society* 332, 951-961